INTEGRATED NORMALCONDUCTING/SUPERCONDUCTING HIGH-POWER PROTON LINAC FOR THE APT PROJECT*

G. P. LAWRENCE and T. P. WANGLER
Los Alamos National Laboratory, Los Alamos NM 87545, USA

Abstract

The baseline accelerator design for the APT (Accelerator Production of Tritium) Project [1] is a normalconducting-superconducting proton linac that produces a CW beam power of 170 MW at 1700 MeV. Compared with the previous all-NC linac design, the NC/SC linac provides significant power savings and lower operating and capital costs. It allows a much larger aperture at high energies, and permits greater operational flexibility. The design has been approved by high-level technical panels and is published in a Conceptual Design Report [2]. The high-energy portion is a superconducting (SC) rf linac employing elliptical-type niobium cavities, while the low-energy portion is a normal-conducting (NC) linac constructed from copper cavities. This provides an integrated accelerator design that makes optimum use of the two technologies in their appropriate regions of application. The NC linac, which consists of an injector, RFQ, CCDTL, and CCL, accelerates a 100-mA beam to 217 MeV. The SC linac is built in two sections optimized for different beam velocity spans, with each section made up of cryomodules containing 5-cell cavities and SC singlet quads in a FODO focusing lattice. Alternate SC linac designs are being studied that employ a doublet focusing lattice using conventional quadrupoles located between cryomodules.

BASELINE NC/SC LINAC DESIGN

The APT linac design is driven strongly by the large amount of rf power required to accelerate the 100-mA CW beam. Efficient conversion is needed at each stage in the power train to minimize capital and operating costs. Parameter selection and cost/performance modeling to achieve this objective have been discussed previously [3]. The current baseline design has evolved from an earlier all-NC linac design [4]. System architecture is displayed in Fig.1, with additional parameters listed in Table 1. The low-energy linac, which is basically the same as in the all-NC design, accelerates a 100-mA proton beam to 217 MeV in copper water-cooled structures. A 75-keV injector housing a microwave-driven ion source generates a continuous 110-mA proton beam. From this input, a 350-MHz, 8-m-long RFQ produces a CW 100-mA beam at 6.7 MeV. The RFQ is built in four resonantly-coupled segments, and rf drive is provided by three 1.2-MW CW klystrons through 12 windows.

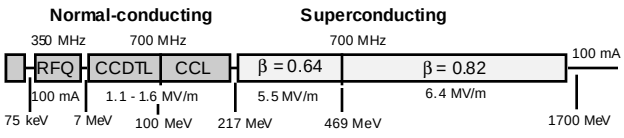

Fig. 1. Architecture of APT integrated NC/SC linac.

The RFQ output is matched into a 700-MHz CCDTL that accelerates it to 100 MeV. The CCDTL is a coupled sequence of 2-gap and 3-gap short DTLs, embedded in an 8-$\beta\lambda$ FODO focusing lattice [5]; the quads are external to the structure. Acceleration continues to 217 MeV in a 700-MHz side-coupled CCL that has the same focusing period. In the CCDTL and CCL, the average accelerating gradient is ramped up to 1.3 MV/m, and accelerating and focusing parameters change smoothly with beta. The result is a linac that has strong focusing at low beam energy and is free from phase-space transitions after the RFQ. Beam dynamics analyses and simulations have shown these factors to be critical in terms of minimizing core emittance growth and the generation of halo [6]. As seen in Table 1, transverse emittance growth is negligible after 20 MeV and longitudinal emittance grows only slightly.

Table 1. NC Low-Energy Linac Parameters

Parameter	RFQ	CCDTL	CCL
Structure gradient (MV/m)	1.38	1.1-1.6	1.6-1.5
Average gradient (MV/m)	1.38	0.4-1.2	1.2-1.3
Length (m)	8.0	102.3	104.3
Synchronous phase (deg)	- (90-33)	- (60-30)	-30
Shunt impedance (MΩ/m)	–	18-52-33	33-37
Phase-adv./period (deg)	–	80	80-35
Quadrupole lattice period		8$\beta\lambda$	8$\beta\lambda$
No. of quadrupoles	–	234	125
Quadrupole G•L prod. (T)		2.6-2.2	2.2-2.0
Trans emitt. (π mm-mrad)*	0.160	0.163	0.163
Long emitt. (π mm-mrad)*	0.405	0.44	0.45
Aperture radius (mm)	2.3-3.4	10-17.5	17.5-25
Aperture : beamsize ratio	–	6.5-14	14-17
Copper rf losses (MW)	1.26	5.0	6.8
Number of klystrons	3	21	27

* Normalized rms values.

The SC high-energy linac consists of a string of cryomodules each containing three or four 5-cell 700-MHz niobium accelerating cavities, alternating with SC quads in a FODO focusing lattice. There are two kinds of cryomodules, each type designed for efficient acceleration in a different velocity range. Cavity shapes [7] in the medium-beta section (217 MeV to 469 MeV) are optimized at β = 0.64, and in the high-beta section at β = 0.82. The shapes are similar to the well-established elliptical designs for electron machines, but are compressed longitudinally in proportion to beta. Because the cavities are short and are driven independently, each section of the SC linac has a broad velocity bandwidth, which allows the gradient profile and output energy to be adjusted over a wide range. Because of the high beam current, the major design push

* Work supported by US Department of Energy

is not for high cavity gradient but high power rf coupler capability. As coupler performance with beam has been demonstrated at about 150 kW and the technology is advancing rapidly, a performance rating of 210 kW has been chosen for the high-β section and 140 kW for the medium-β section. Each cavity is supplied by two antenna-type coaxial couplers mounted on opposite sides of the downstream beam tube. Dual warm coaxial windows are planned, located in the input lines so that they do not see the beam directly.

Fig. 2 sketches the structure of a β=0.82 cryomodule and its rf drive. Each cavity pair is powered by one 1-MW 700-MHz klystron. The quads [8] have SC coils and iron poles, and are similar to the RHIC trim quads. The β=0.64 cryomodules contain three 5-cell cavities, which are powered by one 1-MW klystron, and four SC quads.

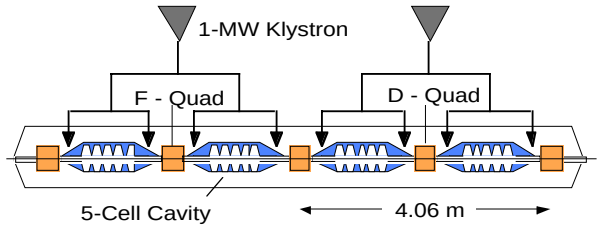

Fig. 2. High-beta cryomodule architecture (β = 0.82)

Table 2. lists key parameters of the two sections of the SC linac. The selection of cavity gradients and numbers of cells per cavity are restricted in both sections by the need to maintain conservative peak surface fields, and power coupler specifications that are close to demonstrated levels. The rf distribution is governed by the need to fully utilize the 840-kW power available from each 1-MW klystron, since the rf system dominates the accelerator cost. A 2K operating temperature for the niobium cavities was chosen to minimize LHe refrigerator and cryodistribution costs. To bound the 2K cryogenic load, the average cavity Q_0 is taken as $5x10^9$, and the static heat leak is estimated at 5 W per meter of cryomodule.

Table 2. Baseline SC High-Energy Linac Parameters

Parameter	**β=0.64**	**β=0.82**
Structure gradient (MV/m)	4.8 - 5.5	5.4 - 6.4
Avg. gradient (MV/m)	1.43-1.51	1.89
Peak surface field (MV/m)	14.9 - 17.1	14.0 - 16.6
Section length (m)	204	792
No. of (5-cell) SC cavities	90	312
No. of klystrons (1-MW)	30	156
Synchronous phase (deg)	-30 to -35	-29
Coupler power (kW)	140	210
Power per klystron (kW)	840	840
Trans. phase adv./period (deg)	83 - 67	81 - 32
Quadrupole length (cm)	30.5	45.9
No. of quadrupoles	120	390
Quadrupole gradient (T/m)	6.4-8.1	5.4
Trans. emittance (π mm-mrad)*	0.16 - 0.17	0.17 - 0.20
Long. emittance (π deg-MeV)*	0.36 - 0.46	0.46 - 1.10
Aperture radius (mm)	65	80
Aperture-radius/rms-beam-size	37 - 56	58 - 85
Thermal load @ 2K (kW)	2.3	11.5

* Normalized rms values.

The key beam dynamics [9] goal for the accelerator is to achieve very low beam losses (0.1 nA/m at 1700 MeV) in order to assure unrestricted hands on maintenance. The NC/SC linac design provides apertures that are much larger than the rms beam size, with the largest apertures at high energies where the activation threat per lost proton is greatest. In the NC linac, the aperture increases in steps to 50 mm, while in the SC linac it jumps to 130 mm at 217 MeV, and then to 160 mm at 469 MeV. Strong transverse focusing keeps the beam size small, and in concert with careful matching, minimizes halo generation. Figure 3 summarizes the result, comparing the linac aperture dimension with both rms beam size and the radius of the outermost trajectories in a 100,000 particle simulation. At full energy, the aperture ratio (ratio of aperture to rms-beam-size) is over 80, at the end of the NC linac it is 17, and at 100 MeV it is 14.

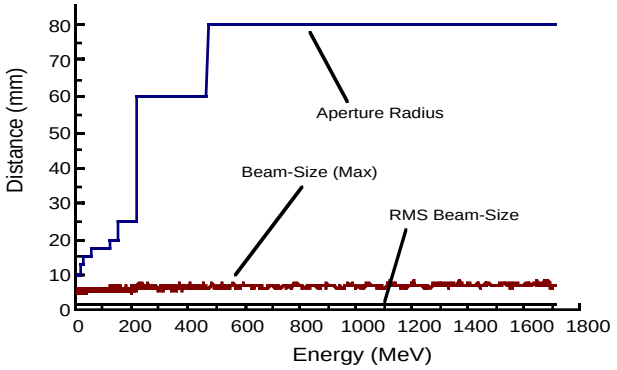

Fig. 3. Aperture radius, rms beam size, & radius of outermost particle for NC/SC baseline linac design.

In order to meet the high availability goal for the accelerator (>85%), redundancy schemes are used to provide excess rf drive in both the NC and SC linacs, but are implemented differently in each. The NC linac is divided into "supermodules" consisting of 100-150 coupled accelerating cells, with each unit supplied by n+1 klystrons (typically 5 to 7), where only n units are needed for operation. When an rf station fails, it is isolated by a waveguide switch, power from the remaining klystrons is increased to compensate, and the supermodule continues to provide the full energy gain needed in that section. In the SC linac, redundancy is provided by including 5% more rf stations and cryomodules than are needed to deliver the nominal 170 MW output power. These are distributed along the high-β linac to compensate for failed units.

Beam simulations show that the SC linac is insensitive to a broad range of construction or operating errors and also can continue to function in a variety of off-normal conditions, including having single klystrons, cavity pairs, and quadrupole pairs out of service. Operational flexibility is enhanced by the retunability of the high-beta section of the SC linac and the adjustability of the cavity gradients.

DOUBLET-LATTICE SC LINAC

The singlet-lattice FODO design for the SC linac meets the performance objectives for APT and provides a very high aperture ratio because of the strong focusing per

unit length. However, because the quadrupoles are inside the cryomodules, construction of these units is complex and relatively expensive. The overall linac architecture is also less than optimum in terms of accessibility of the quads for alignment and space for beam diagnostics. Looking for a better SC linac architecture, we have recently been studying designs based on conventional quadrupole doublets located in the warm regions between cryomodules. This approach simplifies cryomodule construction, shortens the linac by 100 m, reduces the number of quadrupoles, and lowers costs.

Fig. 4 shows the high-β architecture for the alternate SC linac design, and Table 3 summarizes the parameters. Each cryomodule contains 4 cavities, with one klystron driving each cavity pair, using a maximum coupler power of 210 kW. The doublet focusing period is 8.54 m. In the medium-β section, the cryomodules contain two 5-cell cavities, supplied by two power couplers at 124 kW each. A single klystron drives three cavities, so the power of two klystrons is distributed between 3 cryomodules. The doublet period is 4.88 m, providing the relatively strong focusing that the simulations show is needed in this section for good beam control. Beam dynamics for the doublet-based SC linac are discussed in Ref. 9.

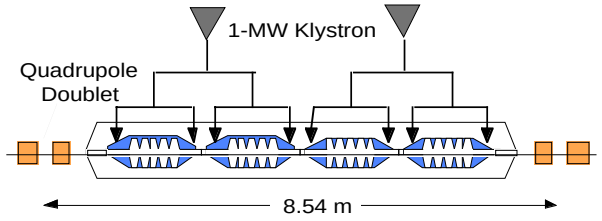

Fig. 4. High-β architecture for doublet-lattice SC linac.

Table 3. Doublet-Lattice SC Linac Parameters

Parameter	**β=0.64**	**β=0.82**
Structure gradient (MV/m)	4.24 - 4.85	5.4 - 6.4
Avg. gradient (MV/m)	1.26	2.25
Peak surface field (MV/m)	13.1 - 15.0	14.0 - 16.6
Section length (m)	249	649
No. of (5-cell) SC cavities	102	304
No. of klystrons (1-MW)	34	152
Synchronous phase (deg)	-30 to -35	-29
Coupler power (kW)	123.5	210
Power per klystron (kW)	741.2	840
Trans. phase adv./period (deg)	83 - 67	81 - 32
No. of quadrupoles	102	152
Trans. emittance (π mm-mrad)	0.17 - 0.18	0.18
Long. emittance (π deg-MeV)	0.34 - 0.33	0.33 - 0.39
Aperture-radius/rms-beam-size	37	65

* Normalized rms values.

A high-β section architecture with only two cavities per cryomodule is also being investigated. The latter has stronger focusing than the 4-cavity unit, because of the shorter period, so the beam size is smaller. However, it makes the linac significantly longer than the FODO baseline and more expensive, because of the larger number of components. Beam simulations without errors show that the rms performance is essentially the same for the 2-cavity and 4-cavity cases. However, error and halo studies must be carried through to provide a more conclusive comparison of the two options, especially with respect to how much beam halo is projected into the high-energy beam transport (HEBT).

OTHER DESIGN ASPECTS AND ED&D

There are several other important aspects of the APT accelerator design (not already referenced) that are covered elsewhere in these Proceedings. These include a description of the rf power system [10], the HEBT and expander system [11], and the accelerator commissioning plan [12].

Engineering development and demonstration programs to confirm design and operation of the major components of the NC/SC linac are well underway. The LEDA program [13], which is prototyping the low-energy linac at full power, has the injector performing at APT specifications, and the RFQ [14] is under construction. For the SC linac, complete cryomodule prototypes will be built and tested prior to industrial production. This step will follow construction and testing of "cryounits" that will integrate 5-cell cavities, power couplers, tuners, and cryostat. Preliminary rf field tests on a single-cell β = 0.64 cavity show no problem in meeting the desired Q_0 vs E specifications. Also, recent proton irradiation measurements on niobium test cavities at Los Alamos and Saclay have put to rest the question of performance reduction at high proton dose levels [15].

REFERENCES

[1] P.W. Lisowski, "The Accelerator Production of Tritium (APT) Project," Proc. 1997 Particle Accelerator Conf., Vancouver (May 1997).

[2] APT Conceptual Design Report, Los Alamos Report LA-UR-97-1329, April 15, 1997.

[3] G.P. Lawrence, et al., " Conventional and Superconducting RF Linac Designs for the APT Project," Proc. 1996 Int. Linac Conf., Geneva, 710 (August 1996).

[4] J.H. Billen et al., "A Versatile High-Power Linac for Accelerator-Driven Transmutation Technologies, Proc. 1995 Particle Accelerator Conf., Dallas, IEEE No. 95CH35843, 1137 (1995).

[5] S. Nath et al., "Physics Design of APT Linac with Normal Conducting rf Cavities," Proc. 1996 Int. Linac Conf., Geneva, Aug 1996.

[6] T.P. Wangler, "New High Power Linacs and Beam Physics Issues," Proc. 1997 Particle Accelerator Conf., Vancouver (May 1997).

[7] F.L. Krawczyk et al., "Superconducting Cavities for the APT Accelerator," ibid.

[8] S. Kahn and P. Wanderer, "Magnetic Design of Superconducting Quadrupoles for a SC Linac for APT," ibid.

[9] S. Nath, et al., "Beam Dynamics Design for the APT Integrated Linac," ibid.

[10] D. Rees, "Design of 250-MW CW RF System for APT," ibid.

[11] R.E. Shafer et al., "Overview of the APT High Energy Beam Transport and Beam Expanders," ibid.

[12] K.C.D. Chan et al., "Commissioning Plan for a High-Current Proton Linac," ibid.

[13] D. Schneider and K.C.D. Chan, "Progress Update on the Low-Energy Demonstration Accelerator," ibid.

[14] D. Schrage et al., "A 6.7-MeV CW RFQ Linac,"

[15] B. Rusnak, et al., "In-situ Proton Irradiation and Measurement of Superconducting RF Cavities under Cryogenic Conditions," ibid